Computational Intelligence in Electrical Engineering
Vol. 16, No. 1, 2025
pp. 15-30
Research Paper

Resilience-Oriented Power Distribution System Planning and Outage Management Based on Operational Situation Awareness

Morteza Haghshenas[1], Rahmatallah Hooshmand*[2]

[1] Assistant professor, Department of Electrical Engineering, Faculty of Engineering, University of Isfahan, Isfahan, Iran
haghshenas.research@gmail.com
[2] Professor, Department of Electrical Engineering, Faculty of Engineering, University of Isfahan, Isfahan, Iran
hooshmand_r@eng.ui.ac.ir

Abstract :
Resilience characteristics in power systems and distribution networks refer to the system's ability to withstand severe disturbances with a low probability of occurrence. This paper proposes a two-level planning framework designed to increase resilience and manage outages in the distribution system by incorporating operational situation awareness. At the first level of the model, decisions are made regarding the allocation of repair crews and emergency generators within the distribution system, and the second stage evaluates the effectiveness of these decisions across various operational scenarios. The actions at the second level include preventive and emergency actions that aim to minimize power outages and the expected costs associated with operating the distribution system. Numerical analyses have been performed using the IEEE 69-bus test system. Simulation results not only validate the model's effectiveness but also demonstrate that integrating operational situation awareness into the resilience planning process significantly mitigates additional investment costs.

Keywords: Distribution system restoration, Emergency operation, Extreme events, Outage management, Preventive operation, Resiliency.

1. Introduction

In recent years, the frequency of extreme weather events (EWEs) has increased due to climate change, and most of these events have been a continual challenge for the electricity infrastructure [1]. Power distribution systems (PDSs) are evolving due to the increasing integration of distributed energy resources and the growing threat of EWEs. Traditional PDS planning methods are insufficient to address these challenges, necessitating a shift towards resilience-oriented PDS planning [2]. PDS resilience is the ability to reduce the magnitude and/or duration of disruptive events, and its effectiveness depends upon its ability to anticipate, absorb, adapt to, and/or rapidly recover

[1] Submission date:09, 04, 2025
Acceptance date:26, 07, 2025
Corresponding author: Rahmatallah Hooshmand, Department of Electrical Engineering, Faculty of Engineering, University of Isfahan, Isfahan, Iran

This is an open access article under the CC BY-NC-ND/4.0/ License (https://creativecommons.org/licenses/by-nc-nd/4.0/).
https://doi.org/10.22108/isee.2025.144861.1729

from a potentially disruptive event [3]. Various approaches, such as both long-term and short-term planning, can be adopted to enhance the resilience of the distribution system [4]. To boost resilience against extreme weather events, it's crucial to revisit long-term planning and system reinforcement as a primary step. A two-stage planning framework found in the literature is illustrated in Fig. 1. In the first stage, expansion and reinforcement actions, including distribution line hardening [5-17], distribution substation hardening [18-19], distributed generator (DG) placement [5-8], [11], [14-17], and remote controlled switch (RCS) placement [6-7], [15-16], [20], are determined. In the second stage, emergency operations following disruptions are simulated to assess the effectiveness of the strategies for expansion and reinforcement from the first stage. This effectiveness is evaluated based on emergency operation costs, including costs related to load shedding, restoration, etc. The actions that can be adopted in the second stage include load shedding [5-18], [20], network reconfiguration [5-7], [11], [15-18], DG dispatching [5-18], microgrid formation [5], [10], [20-22], repairing [5-7], [9], [15-18], [22-24], and repair crew (RC) scheduling [5], [17], [25-26]. Additionally, during the second stage, constraints linked to network power flow are applied. A typical objective function is to minimize both investment and emergency operation costs.

To address uncertainties, stochastic and robust modeling techniques are employed. As illustrated in Fig. 1, the stochastic approach [27] represents the second stage of planning using independent scenarios, each with a defined probability of happening. Each scenario reflects a feasible outcome of the uncertainty factors, including equipment damage (due to the EWEs), repair duration, load, and renewable DG generation. Furthermore, the anticipated costs of emergency operations based on these scenarios are integrated as the second-stage cost in the objective function. In contrast, the robust approach [8-10], [12-14], [28], as depicted in Fig. 1, frames the second stage through a bi-level optimization aimed at identifying the most detrimental equipment outages. Here, the expenditures associated with the emergency operation period tied to the worst outages are considered the second-stage cost in the objective function.

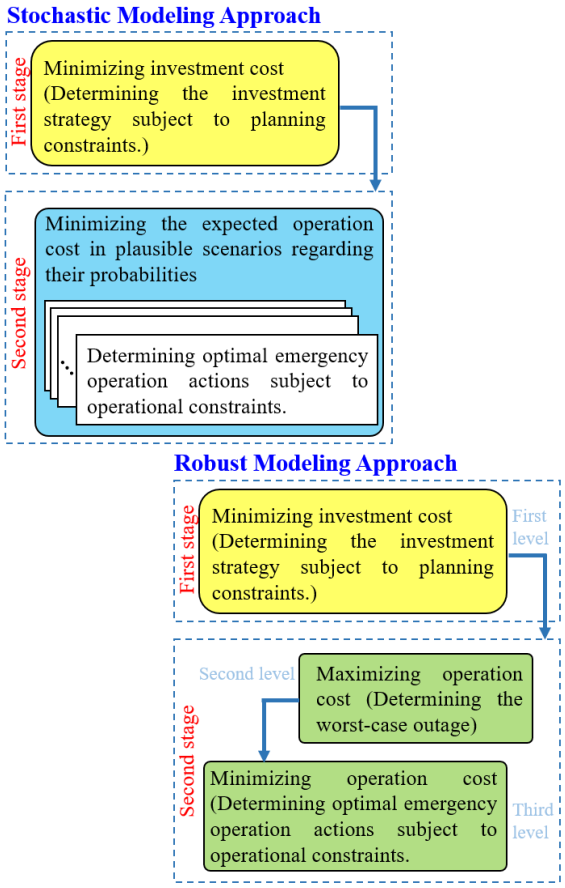

Fig. 1. PDS resilience planning frameworks.

Situational awareness is generally understood as "the recognition of elements in the environment over a specific time and space, understanding their significance, and anticipating their future conditions" [29-30]. With technological advancements and mathematical modeling, the occurrence and impacts of EWEs can often be predicted from seconds to hours in advance, depending on the type of event [31]. Thus, forecasts of EWEs (such as hurricane trajectory and wind intensity) combined with the current and projected future conditions of power distribution systems (PDSs) equip the distribution network operator (DNO) with operational situational awareness (OSA) regarding EWEs. This capability enables the DNO to strategize effectively in preparation for upcoming events. The DNO could prepare the system for the upcoming event, for example, by preparing the crew and the required equipment [4-5], and pre-allocation of DGs to enhance the system's resilience.

In the reviewed literature, the effectiveness of

a PDS resilience enhancement strategy is assessed by its ability to reduce the impacts of EWEs. Within these models, the PDS's resilience against EWEs is gauged by the degradation of system performance during such events. However, in the case of EWEs, the DNO, due to its OSA, can take necessary measures to effectively address the impending events. Ignoring this capability in the resilience evaluations leads to an underestimation of the PDS's resilience. Implementing expansion planning measures grounded in this underestimated resilience leads to increased costs for reinforcement and expansion. Conversely, recognizing the influence of situational awareness in the planning framework enables a more strategic investment approach. This paper seeks to address the research gap by proposing a novel resilience-oriented PDS planning and outage management model based on DNO's OSA. To sum up, the key contributions of the proposed model are as follows:

- A novel technique is proposed to joint resilience-oriented PDS planning and outage management considering the impact of the DNO's situational awareness.
- Coordinating RC dispatch and distribution network reconfiguration to reduce the number of decision variables by redefining outage management constraints.
- Modeling the proposed technique as a bi-level stochastic mixed integer linear programming (MILP) problem that can be efficiently solved using available commercial software (e.g., GAMS).

The remainder of the paper is organized as follows. Section 2 presents the problem statement. Section 3 describes the mathematical formulation of the proposed model. Section 4 presents the simulation results and discusses the effectiveness of the proposed model. Finally, Section 5 concludes the paper.

2. Proposed Framework

The proposed framework for resilience-oriented PDS planning and outage management considering the impact of the DNO's situational awareness is shown in Fig. 2. Based on the pros and cons of the two modeling techniques outlined in Section 1, the stochastic method is utilized. This approach can effectively capture the influence of EWEs and the specific geographic characteristics of the PDS on potential system damage. As illustrated in Fig. 1, the stochastic modeling approach assesses the effectiveness of each investment plan aimed at enhancing PDS resilience by simulating actions taken during emergency operations under various plausible scenarios. Investment plans that achieve lower costs while yielding higher expected resilience metrics are prioritized. Each scenario presents a likely EWE and the PDS condition post-event. With the DNO's situational awareness regarding EWEs, the DNO can ready the PDS upon receiving alerts of an approaching EWE. To account for this readiness, we define this preparatory timeframe for each scenario as the preventive operation period. As illustrated in the proposed framework in Fig. 2, the effectiveness of each investment strategy is assessed through simulations of two consecutive operational periods: preventive and emergency. Thus, the significance of the DNO's situational awareness in assessing investment strategies is taken into account.

Decision variables in the first stage of the proposed model are to locate emergency DGs and determine the number of RCs and equip them for PDS restoration, subject to budget constraints. The second stage assesses the PDS resilience for each scenario. Each scenario comprises two time frames. The first timeframe simulates the DNO's situational awareness, in which the DNO readies the system to better adapt to forthcoming events based on the available EWE information, referred to as the preventive operation period. The DNO decision variables during this period include determining hourly switch statuses for network reconfiguration, dispatching DGs, and managing RCs. Upon the occurrence of an EWE, the second timeframe, or emergency operation period, commences. During this period, the DNO attempts to supply more loads and minimize the expected costs of energy not supplied and repair costs by implementing corrective actions. Decision variables here involve determining switch statuses for network reconfiguration, dispatching DGs, managing RCs, and load shedding. The operational constraints remain in effect throughout both periods. The sources of uncertainty stem from PDS load, the condition of distribution lines, and the time required for their repair. The uncertainties stem from PDS load, distribution lines damage status, and the time required for their repair.

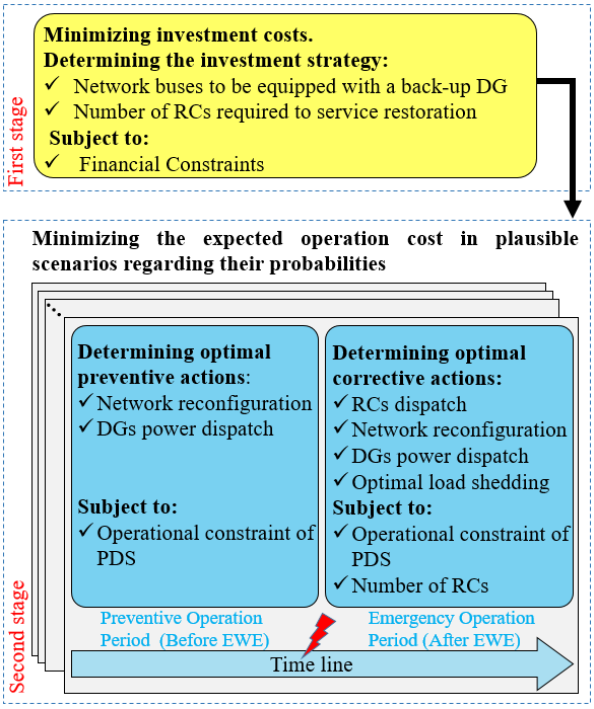

Fig. 2. The proposed model.

In the proposed model, the restoration time of damaged lines in each scenario is a random variable that depends on three factors: availability of RCs, the time to arrive at the affected location, and the time required to repair the line [5-6]. As shown in Fig. 3, when line *l* is damaged by EWE, a "waiting time" may be required to dispatch one of the RCs to the damaged location. The waiting time depends on the number of RCs, the number of damaged lines, the repair priority of the lines, and the repair time. The waiting time for the damaged line *l* starts from the time of damage and continues until one of the RCs is dispatched to that line. In the case of EWE, the first failure is reported for line *l* in the PDS, and one of the RCs is immediately dispatched from the depot to the line location for repair. In such a situation, the waiting time for line *l* is zero, and the restoration process starts when an RC reaches the location of the damaged line *l*.

With the increase in the number of EWE-induced line failures, each RC has to restore more than one damaged line. Therefore, when RC(*c*) is busy repairing line *l*, the waiting time for other damaged lines that are supposed to be restored by RC(*c*) is non-zero. In this situation, the waiting time is longer for the damaged line whose restoration is less important, and DNO has preferred to use RC(*c*) to restore more important lines. After an RC is dispatched to repair line *l*, the travel time for the RC to arrive at the affected location on line *l* is denoted by $T_l^T(s)$. The travel time between two damaged lines or between the depot and a damaged line can be obtained using the geographic information system. In practice, the time it takes for an RC to travel between two points in the PDS depends on some uncertain parameters, such as the traffic on the route. Therefore, in the proposed model, uncertainties in the time of traveling between different PDS points in each scenario can be included in parameter $T_l^T(s)$. Moreover, the modeling of $T_l^T(s)$ during the restoration of damaged lines makes possible the use of the proposed model in resilience improvement planning of georeferenced PDSs. Once an RC arrives at a damaged line *l*, they spend time $T_l^R(s)$ to repair the damaged line, and then, they are dispatched to the next damaged line.

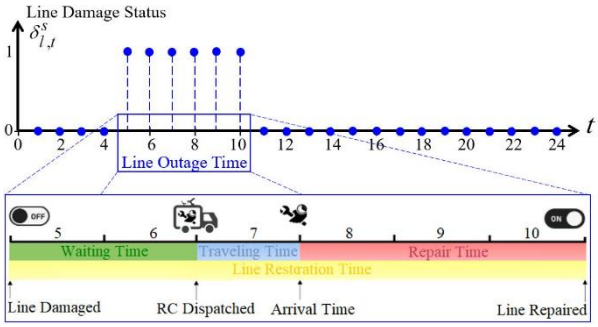

Fig. 3. Time sequence of the distribution line outage duration.

For example, the damage status of line *l* in a scenario is shown in Fig. 3. As can be seen, this line fails due to EWE at t=5, and no RC is free until t=7. At t=7, an RC is dispatched to the damaged line location, and since $T_l^T(s)=1$, the RC arrives an hour later. The repair process starts at t=8 and finishes at t=10. Finally, at t=11, line *l* is repaired. In this paper, it is assumed that $T_l^R(s)$ for each damaged line is independent and shares the same probability density function [5].

3. Mathematical Formulation

3.1. Objective Function

The objective function of the proposed model is introduced in (1). It is composed of two terms: annualized investment cost and expected operation cost.

$$\min \left\{ C_I + D \sum_{s \in \partial^S} p(s) C_o(s) \right\} \quad (1)$$

The first term in (1) reflects the investment costs related to providing RCs and installing DGs, calculated as (2).

$$C_I = \zeta^{rc} C^{RC} + \sum_{n \in \partial^G} \zeta_n^g C^{DG} \quad (2)$$

where $\zeta^{rc} \in \mathrm{N}$ is the number of RCs required for optimal outage management. The number of RCs depends on the EWE severity and the damage status of distribution lines in the operation scenarios. A DG will be installed on bus *n* ($\zeta_n^g = 1$) if the expected annual outage cost of bus *n* in the operation scenarios is greater than the annualized cost of installing the DG. Furthermore, in practice, the operating costs of DGs also affect the decision whether to install them in PDS. The operation cost in each scenario to calculate the second term in (1), which is composed of expected cost of energy not supplied and the repairing cost during the event, is defined as in (3).

$$C_o(s) = [\sum_{n \in \partial^L} \sum_{t \in \partial^{Te}} C_n^L \alpha_n^L \gamma_{n,t}^{L,s} P_{n,t}^{L,s} + \sum_{n \in \partial^{PCC}} \sum_{t \in \partial^{Te}} C_n^{gr} P_{n,t}^{gr,s} + \sum_{n \in \partial^G} \sum_{t \in \partial^{Te}} C_n^g P_{n,t}^{g,s} + \sum_{l \in \partial^B} \sum_{t \in \partial^{Te}} C_l^r \tau_{l,t}^{r,s}] \Delta t \quad (3)$$

where

$$C_n^L = x_n^{IL} C^{IL} + x_n^{RL} C^{RL} + x_n^{CL} C^{CL} \ , \forall n \in \partial^L \quad (4)$$

$$x_n^{IL} + x_n^{RL} + x_n^{CL} = 1 \ , \forall n \in \partial^L \quad (5)$$

In the objective function (3), α_n^L is load importance factor at bus *n* and its value may differ across load buses. Also, $\tau_{l,t}^{r,s}$ is a binary variable and its value is 1 when an RC is dispatched to repair line *l* and remains 1 until the end of the repair of the line. In other words, the value of this variable for line *l* remains 1 for $T_l^T(s) + T_l^R(s)$ hours. This timeframe should not be mistaken for the outage duration of line *l*. In reality, this timeframe represents the shortest outage duration of line *l* and could extend based on the number of RCs and the repair priorities assigned to line *l*. In the proposed framework, the priority for repairing damaged lines is determined based on the expected outage costs resulting from their damage. This means that the greater the expected outage cost due to damage in a distribution line, the more pressing the need becomes to repair that line. Effective outage management during and following EWEs requires the creation of a mathematical model that correlates the ON-OFF state of lines with the performance metrics of RCs. To achieve this, three key challenges arise: 1) RCSs are present only on specific lines, complicating the isolation of damaged segments while minimizing power outages. 2) The decisions made in the second stage, which include RCS status and RC dispatch, are interconnected, and the dependency of this variable on first-stage decisions adds to the modeling complexity of outage management. 3) When coordinating RC dispatch for the repair of damaged lines and reconfiguring the network, the radiality constraints of the PDS must be satisfied. This paper tackles these challenges.

3.2. First Stage Constraints

The planning measures are influenced by financial budgets, according to (6)-(8).

$$\zeta^{rc} C^{RC} \le B_{rc} \quad (6)$$

$$\sum_{n \in \partial^G} \zeta_n^g C^{DG} \le B_{dg} \quad (7)$$

$$C_I \le B_R \quad (8)$$

Constraints (6) and (7) represent optional financial budget limits, allowing planners to choose any combination depending on the circumstances. Meanwhile, constraint (8) constrains the overall investment costs to the budget set aside for enhancing PDS resilience.

3.3. Preventive Operation Period Constraints

During the preventive and emergency operation periods, we consider all constraints as $\forall s \in \partial^S$. This will not be explicitly mentioned when laying out the subsequent constraints. In the proposed framework, the decision variable $\chi_{l,t}^{r,s} \in \{0,1\}$ governs the *ON* (1) or *OFF* (0) statuses of RCSs. Constraint (9) stipulates that an RCS on line *l* can only be activated if the line is equipped with RCS. Meanwhile, binary variable $\pi_{l,t}^s$, outlined in constraint (10), specifies the *ON-OFF* status of line *l* at time *t*. During the preventative operational period, line *l* remains intact at time *t* ($\delta_{l,t}^s = 0$), keeping its status as *ON* (energized). Constraint (12) complements constraints (10) and (11) to establish the *ON* or *OFF* statuses of the lines.

$$\chi_{l,t}^{r,s} \le \phi_l^r \quad \forall l \in \partial^{SW}, t \in \partial^{T_p} \tag{9}$$

$$\chi_{l,t}^{r,s} + \pi_{l,t}^s \le 1 \quad \forall l \in \partial^B, t \in \partial^{T_p} \tag{10}$$

$$\pi_{l,t}^s \le 1 \quad \forall l \in \partial^B, t \in \partial^{T_p} \tag{11}$$

$$\chi_{l,t}^{r,s} + \phi_l^r + 2\pi_{l,t}^s \ge 2 \quad \forall l \in \partial^B, t \in \partial^{T_p} \tag{12}$$

Constraints (13) and (14) define the active and reactive power flows of distribution lines. If $\pi_{l,t}^s = 0$, the state of line l is OFF, and there is no power flow through the line.

$$-\pi_{l,t}^s.P_l^{\max} \le P_{l,t}^s \le \pi_{l,t}^s.P_l^{\max} \quad \forall l \in \partial^B, t \in \partial^{T_p} \tag{13}$$

$$-\pi_{l,t}^s.Q_l^{\max} \le Q_{l,t}^s \le \pi_{l,t}^s.Q_l^{\max} \quad \forall l \in \partial^B, t \in \partial^{T_p} \tag{14}$$

Constraints (15)-(19) delineate the linearized dist-flow equations, which are extensively utilized in the planning and operation of radial PDSs [6-7]. Specifically, constraints (15) and (16) encapsulate the active and reactive power balance equations, where $l \in \partial^B$ indicates a line connecting bus n to bus m, and $l' \in \partial^B$ denotes a line linking bus m to bus n. The network's connectivity, governed by the *ON-OFF* status of the lines, is represented through constraints (13)-(18). This paper employs the big-M method to guarantee the voltage separation of two unlinked buses. Constraint (19) establishes the permissible range for voltage deviations.

$$\sum_{\{m|l\in\partial^B\}} P_{l,t}^s + (1-\gamma_{n,t}^{L,s})P_{n,t}^{L,s} = \sum_{\{m|l'\in\partial^B\}} P_{l',t}^s + P_{n,t}^{g,s} \quad \forall n \in \partial^N, t \in \partial^{T_p} \tag{15}$$

$$\sum_{\{m|l\in\partial^B\}} Q_{l,t}^s + (1-\gamma_{n,t}^{L,s})Q_{n,t}^{L,s} = \sum_{\{m|l'\in\partial^B\}} Q_{l',t}^s + Q_{n,t}^{g,s} \quad \forall n \in \partial^N, t \in \partial^{T_p} \tag{16}$$

$$v_{m,t}^s - v_{n,t}^s + \frac{R_l P_{l,t}^s + X_l Q_{l,t}^s}{V_0} \le (1-\pi_{l,t}^s)M \quad \forall (n,m) \in \partial^N, l \in \partial^B, t \in \partial^{T_p} \tag{17}$$

$$v_{m,t}^s - v_{n,t}^s + \frac{R_l P_{l,t}^s + X_l Q_{l,t}^s}{V_0} \ge (\pi_{l,t}^s - 1)M \quad \forall (n,m) \in \partial^N, l \in \partial^B, t \in \partial^{T_p} \tag{18}$$

$$V_0 - \Delta v \le v_{n,t}^s \le V_0 + \Delta v \quad \forall n \in \partial^N, t \in \partial^{T_p} \tag{19}$$

Constraints (20) and (21) limit the active and reactive powers of DG at bus n if it has been allocated in the first stage.

$$\zeta_n^g.P_n^{g,\min} \le P_{n,t}^{g,s} \le \zeta_n^g.P_n^{g,\max} \quad \forall n \in \partial^G, t \in \partial^{T_p} \tag{20}$$

$$\zeta_n^g.Q_n^{g,\min} \le Q_{n,t}^{g,s} \le \zeta_n^g.Q_n^{g,\max} \quad \forall n \in \partial^G, t \in \partial^{T_p} \tag{21}$$

The radiality constraints for network reconfiguration are enforced by (22)-(24), which are based on the spanning tree approach [6]. Constraint (22) represents the relation between the ON-OFF status of the lines and the spanning tree variables $\omega_{nm,t}^s$ and $\omega_{mn,t}^s$, regardless of the power flow direction. According to (22), line l at time t is in the spanning tree $(\pi_{l,t}^s = 1)$ if either bus n is the parent of bus m $(\omega_{nm,t}^s = 1)$, or bus m is the parent of bus n $(\omega_{mn,t}^s = 1)$. Constraint (23) requires that every bus other than the point of common coupling (PCC) should have at most one parent bus, while (24) indicates that the PCC has no parent.

$$\omega_{nm,t}^s + \omega_{mn,t}^s = \pi_{l,t}^s \quad \forall l \in \partial^B, t \in \partial^{T_p} \tag{22}$$

$$\sum_{m\in N(n)} \omega_{nm,t}^s \le 1 \quad \forall n \in \partial^N, t \in \partial^{T_p} \tag{23}$$

$$\omega_{nm,t}^s = 0 \quad \forall (n,m) \in \partial^{PCC}, t \in \partial^{T_p} \tag{24}$$

Constraints (25) and (26) limit the active and reactive powers exchanged with the upstream network in the preventive operation period.

$$0 \le P_{n,t}^{gr,s} \le P_l^{gr,\max} \quad \forall n \in \partial^{PCC}, t \in \partial^{T_p} \tag{25}$$

$$-Q_l^{gr,\max} \le Q_{n,t}^{gr,s} \le Q_l^{gr,\max} \quad \forall n \in \partial^{PCC}, t \in \partial^{T_p} \tag{26}$$

3.4. Emergency Operation Period Constraints

During the emergency operational period, if line l is damaged at time t $(\delta_{l,t}^s = 1)$, it is compulsorily OFF at this time. Constraint (30) aids in defining the ON or OFF statuses of lines in conjunction with constraints (28) and (29). Constraints (31) and (32) govern the power flows in distribution lines. The linearized dist-flow equations are outlined by constraints (33)-(37). Constraints (38) and (39) restrict the output power of DG at bus n. Radiality is maintained through constraints (40)-(42), while constraints (43) and (44) cap the power exchanged with the upstream power system during emergency operations. In the proposed

model, the restoration of damaged lines is implemented to minimize load shedding costs while considering the number of RCs established in the initial stage. Constraint (45) ensures that RCs are limited to repairing just one line at time *t*. Based on constraint (46), only one RC can be assigned to repair a specific damaged line. In constraints (47) and (48), $\chi_{c,l,t}^{on,s} \in \{0,1\}$ signifies when RC(c) initiates the repair of line *l*. Additionally, $\chi_{c,l,t}^{off,s} \in \{0,1\}$ specifies when RC(*c*) finishes repairing line *l*. In constraint (47), the parameters $\chi_{c,l,t}^{on,s}$ and $\chi_{c,l,t}^{off,s}$ are established based on the variations of $\chi_{c,l,t}^{s}$ over time. Per constraints (49) and (50), an RC is permitted to begin repairs on a damaged line only if it was selected and equipped during the first stage. Constraint (51) mandates that repairs for a damaged line must be carried out continuously from the time the RC arrives. As stated in constraint (52), $\chi_{c,l,t}^{off,s} \in \{0,1\}$ indicates the maximum duration allowed for an RC to complete the repair. Constraint (53) represents the load shedding ratio limit. The load shedding is modeled as a continuous variable to reflect the effect of the proposed preventive and corrective actions.

$$\chi_{l,t}^{r,s} \le \phi_l^r \qquad \forall l \in \partial^{SW}, t \in \partial^{T_e} \tag{27}$$

$$\chi_{l,t}^{r,s} + \pi_{l,t}^{s} \le 1 \qquad \forall l \in \partial^{B}, t \in \partial^{T_e} \tag{28}$$

$$\pi_{l,t}^{s} + \delta_{l,t}^{s} \le 1 \qquad \forall l \in \partial^{B}, t \in \partial^{T_e} \tag{29}$$

$$\chi_{l,t}^{r,s} + \phi_l^r + 2(\pi_{l,t}^{s} + \delta_{l,t}^{s}) \ge 2 \quad \forall l \in \partial^{B}, t \in \partial^{T_e} \tag{30}$$

$$-\pi_{l,t}^{s}.P_l^{\max} \le P_{l,t}^{s} \le \pi_{l,t}^{s}.P_l^{\max} \quad \forall l \in \partial^{B}, t \in \partial^{T_e} \tag{31}$$

$$-\pi_{l,t}^{s}.Q_l^{\max} \le Q_{l,t}^{s} \le \pi_{l,t}^{s}.Q_l^{\max} \quad \forall l \in \partial^{B}, t \in \partial^{T_e} \tag{32}$$

$$\sum_{\{m|l\in\partial^B\}} P_{l,t}^{s} + (1-\gamma_{n,t}^{L,s})P_{n,t}^{L,s} = \sum_{\{m|l'\in\partial^B\}} P_{l',t}^{s} + P_{n,t}^{g,s} \qquad \forall n \in \partial^{N}, t \in \partial^{T_e} \tag{33}$$

$$\sum_{\{m|l\in\partial^B\}} Q_{l,t}^{s} + (1-\gamma_{n,t}^{L,s})Q_{n,t}^{L,s} = \sum_{\{m|l'\in\partial^B\}} Q_{l',t}^{s} + Q_{n,t}^{g,s} \qquad \forall n \in \partial^{N}, t \in \partial^{T_e} \tag{34}$$

$$v_{m,t}^{s} - v_{n,t}^{s} + \frac{R_l P_{l,t}^{s} + X_l Q_{l,t}^{s}}{V_0} \le (1-\pi_{l,t}^{s})M \qquad \forall (n,m) \in \partial^{N}, l \in \partial^{B}, t \in \partial^{T_e} \tag{35}$$

$$v_{m,t}^{s} - v_{n,t}^{s} + \frac{R_l P_{l,t}^{s} + X_l Q_{l,t}^{s}}{V_0} \ge (\pi_{l,t}^{s} - 1)M \qquad \forall (n,m) \in \partial^{N}, l \in \partial^{B}, t \in \partial^{T_e} \tag{36}$$

$$V_0 - \Delta v \le v_{n,t}^{s} \le V_0 + \Delta v \quad \forall n \in \partial^{N}, t \in \partial^{T_e} \tag{37}$$

$$\zeta_n^g.P_n^{g,\min} \le P_{n,t}^{g,s} \le \zeta_n^g.P_n^{g,\max} \quad \forall n \in \partial^{G}, t \in \partial^{T_e} \tag{38}$$

$$\zeta_n^g.Q_n^{g,\min} \le Q_{n,t}^{g,s} \le \zeta_n^g.Q_n^{g,\max} \quad \forall n \in \partial^{G}, t \in \partial^{T_e} \tag{39}$$

$$\omega_{nm,t}^{s} + \omega_{mn,t}^{s} = \pi_{l,t}^{s} \quad \forall l \in \partial^{B}, t \in \partial^{T_e} \tag{40}$$

$$\sum_{m\in N(n)} \omega_{nm,t}^{s} \le 1 \qquad \forall n \in \partial^{N}, t \in \partial^{T_e} \tag{41}$$

$$\omega_{nm,t}^{s} = 0 \qquad \forall (n,m) \in \partial^{PCC}, t \in \partial^{T_e} \tag{42}$$

$$0 \le P_{n,t}^{gr,s} \le P_l^{gr,\max} \quad \forall n \in \partial^{PCC}, t \in \partial^{T_e} \tag{43}$$

$$-Q_l^{gr,\max} \le Q_{n,t}^{gr,s} \le Q_l^{gr,\max} \quad \forall n \in \partial^{PCC}, t \in \partial^{Te} \tag{44}$$

$$\sum_{l\in\partial^B} \chi_{c,l,t}^{s} \le 1 \qquad \forall c \in \partial^{C}, t \in \partial^{T_e} \tag{45}$$

$$\sum_{c\in\partial^C} \chi_{c,l,t}^{s} \le 1 \qquad \forall l \in \partial^{B}, t \in \partial^{T_e} \tag{46}$$

$$\chi_{c,l,t}^{on,s} - \chi_{c,l,t}^{off,s} = \chi_{c,l,t}^{s} - \chi_{c,l,(t-1)}^{s}, \qquad \forall c \in \partial^{C}, l \in \partial^{B}, t \in \partial^{T_e} \tag{47}$$

$$\chi_{c,l,t}^{on,s} + \chi_{c,l,t}^{off,s} \le 1 \qquad \forall c \in \partial^{C}, l \in \partial^{B}, t \in \partial^{T_e} \tag{48}$$

$$\chi_{c,l,t}^{on,s} \le Z_c^{RC} \qquad \forall c \in \partial^{C}, l \in \partial^{B}, t \in \partial^{T_e} \tag{49}$$

$$\sum_{c\in\partial^C} Z_c^{RC} \le \zeta^{rc} \tag{50}$$

$$\sum_{c\in\partial^C} \sum_{t\in\partial^{T_e}} \chi_{c,l,t}^{on,s} + \chi_{c,l,t}^{off,s} \le 2 \qquad \forall l \in \partial^{B} \tag{51}$$

$$\sum_{t\in\partial^{T_e}} \sum_{l\in\partial^B} \chi_{c,l,t}^{s} \le T_c^{\max} \qquad \forall c \in \partial^{C} \tag{52}$$

$$0 \le \gamma_{n,t}^{L,s} \le 1 \qquad \forall n \in \partial^{L}, t \in \partial^{T_e} \tag{53}$$

3.5. Solution Methodology

In this paper, the stochastic scenarios generation process and determining the damage status of distribution lines will be carried out independently from the proposed planning model. With the damage status of the lines established for each scenario, the compact representation of the first stage problem can be articulated as follows:

$$\min_x \left\{ Z_1^T x + \psi(x) : Ax \le B \right\} \tag{54}$$

Here, the vector Z_1 indicates the cost coefficients for enhancing PDS resilience, while vector *x* denotes the decisions made in the first stage, and $\psi(x) = \sum_s [P(s).u(x,s)]$ refers to the recourse function of the second stage, which calculates the expected value based on the decision *x*. The resilience budget in vector form for the first stage is provided in (54). The value function for the second stage, denoted as $u(x,s)$ for a specific scenario, is defined as follows:

$$\min\left\{Z_2^T y : W.y \le E(s) - F(s).x\right\} \quad (55)$$

The objective function in (55) encapsulates the compact form of the objective function (3), with vector *y* representing the decisions made in the second stage. The second stage constraints (9)-(53) can be represented in vector form as indicated in (54). The parameters Z_1, A, B, Z_2, W, E, and F constitute the input data for the proposed model. The model in the format of (54)-(55) presents an optimization problem solvable via a standard MIP solver, such as CPLEX.

4. Simulation Results

In this section, the numerical results of the proposed model are obtained for the IEEE 69-bus test system. In the scenario generation process, it is assumed that the total operating time of PDS lasts 24 hours on average. The proposed model identifies three sources of uncertainty: hourly load, repair time of distribution lines, and the lines' damage status. In this paper, PDS loads are categorized into three sectors: industrial, commercial, and residential. Fig. 4 shows the multipliers of industrial, commercial, and residential load profiles at a substation on a typical day in summer [32]. The active and reactive loads are normalized with respect to their peak values, respectively. We assume a homogeneous load pattern: all individual node loads share the same normalized load profiles [7]. The base values of each load are given by the test system. Consequently, the load for each bus at every hour is calculated based on the base load at that bus, the load multiplier from the daily load profile, and a random coefficient following a normal distribution $N(1,0.1^2)$ [7]. Also, it is assumed that all buses other than PCC are candidates for DG installation. The Weibull distribution function with *k=10* and *y=2* is used to calculate the random time of distribution line repair [6]. In the first stage of the proposed model, the annualized investment costs considering the lifetime of the equipment and a discounting rate of 3.5% [33] are listed in Table 1, and other parameters are listed in Table 2. In practice, the distance between the distribution lines in PDS is short, so, in the present study, the value of $T_l^T(s)$ is assumed to be 1 while the generality of the problem is maintained in all scenarios.

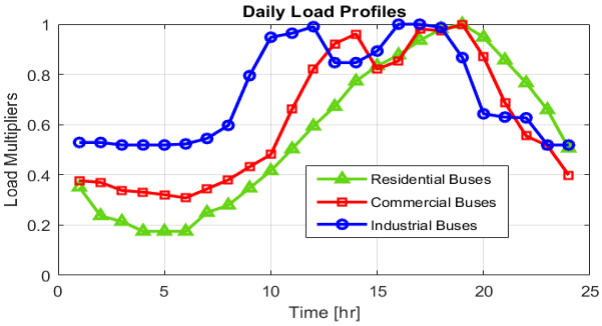

Fig. 4. Distribution system daily load profiles [33].

Table 1. The annualized cost of strategies in the first stage.

strategy	Capital cost($)	Life time (years)	Annualized cost ($)
DG	400,000 [15]	50	8,527
RC	112,000 [5]	25	12,863

Table 2. The PDS operation parameters in the second stage.

Par.	Value	Par.	Value
C^{IL}	9.085 $/kwh [33]	C^r	200 $/hr [6]
C^{CL}	8.552 $/kwh [33]	$P^{g,max}$	400 kw [5]
C^{RL}	0.482 $/kwh [33]	$Q^{g,max}$	300kvar [5]
C^g	7.5 ¢/kwh [5]	V_0	1 p.u
C^{gr}	6.5 ¢/kwh [33]	Δv	0.05 p.u
Δt	1 hr	D	3
T_c^{max}	20 hr		

Simulations are performed in two cases so that the efficiency of PDS resilience strategies can be evaluated. In case 1, the number of required RCs is determined based on the PDS lines' damage status. In this case, DGs are allocated to reduce the load shedding. In case 2, the effect of network reconfiguration on resilience-oriented PDS planning and operation is evaluated. The proposed model was executed on a PC with a 3.2-GHz Intel Core (TM) i7-6900K processor and 128GB RAM. Moreover, the model was solved using the CPLEX solver under the GAMS optimization package.

According to the baseline simulation results, when no measures are taken to improve the PDS resilience, the total expected operating cost is $303,003, and the expected energy not supplied (EENS) is more than 12,041 kWh. The preventive and emergency operation periods are considered to be 4 and 20 hours, respectively. This indicates that the DNO is notified of the EWE four hours early and starts taking preventive measures based on its knowledge of the PDS. The RCS's location and lines damage status in the worst EWE

scenario are presented in Fig. 5, and the resilience-oriented PDS planning results in cases 1-2 are presented in Table 3. Fig. 6 illustrates the PDS outage management during the emergency operation period and the impact of RC dispatch on the service restoration process. As depicted in Fig. 6, the emergency operation period has started after the damage of the first distribution line. In Case 1, since the DNO is not allowed to network reconfiguration, switches S1 to S8 are all in the closed state, and tie-switches T1 to T4 are all in the open state. This structure is the optimal structure for operating the IEEE 69-bus PDS under normal conditions with all network buses connected to the PCC. Also, as shown in Fig. 7, in case 1, five DGs have been installed in buses 57, 60, 61, 64, and 65 to alleviate load shedding costs during emergencies and are prepared for operation. During the emergency operation period, RCs focus on repairing the damaged lines according to their significance in minimizing expected operational costs. Consequently, the line that most significantly contributes to lowering operating costs is prioritized for earlier repair.

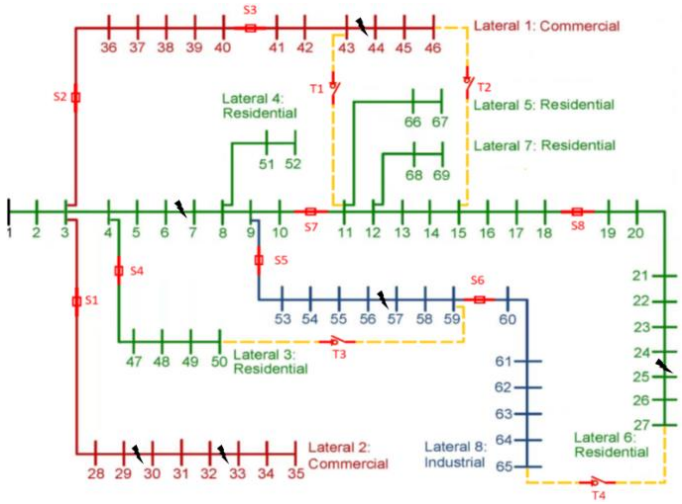

Fig. 5. The lines damage status in the worst scenario.

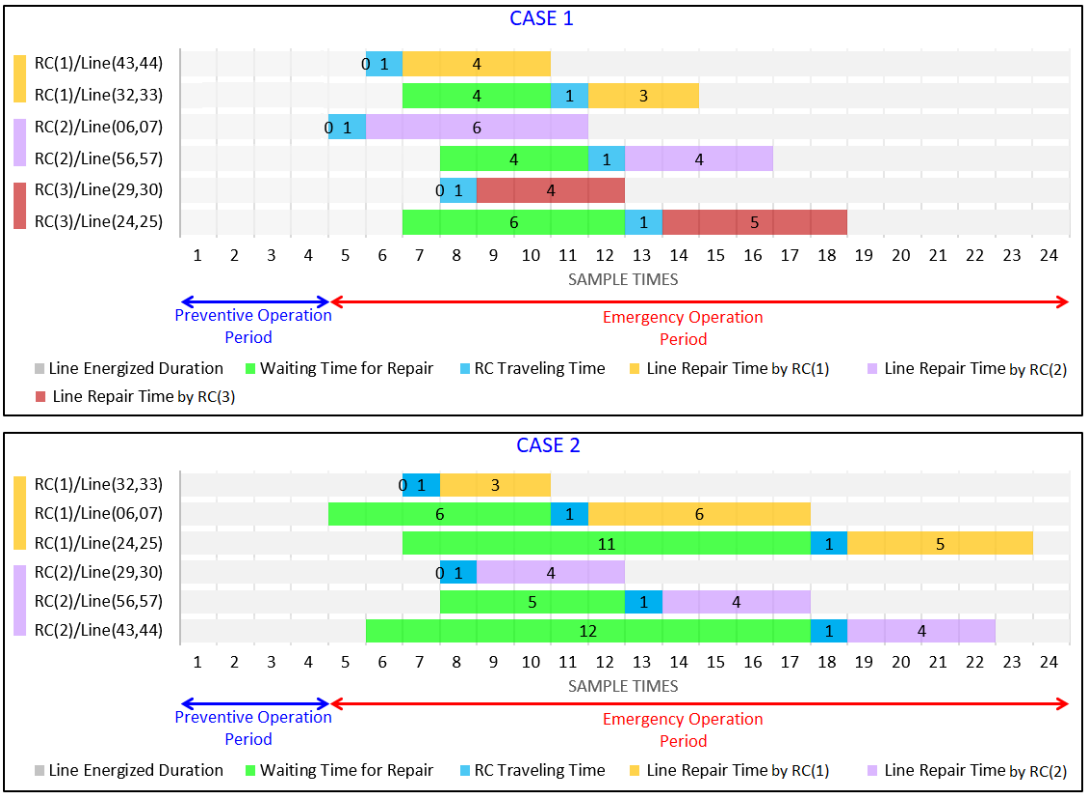

Fig. 6. IEEE 69-bus PDS service restoration process in the emergency operation period.

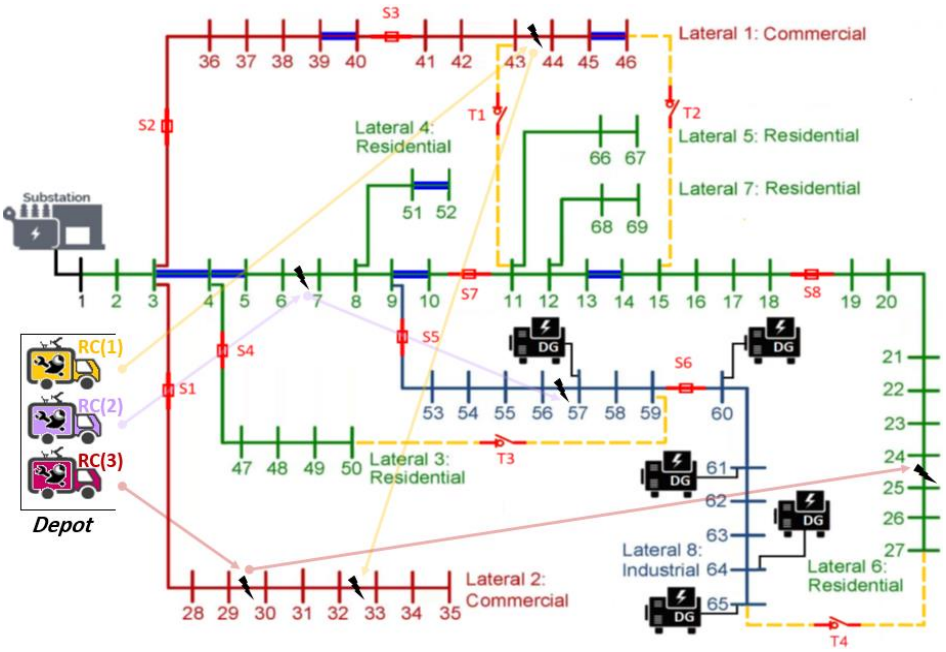

Fig. 7. IEEE 69-bus PDS planning results of case 1.

Table 3. The planning results for IEEE 69-bus PDS.

Planning results	Case 1	Case 2
Allocated RCs	3	2
Allocated DGs	5	1
Investment costs ($)	81,224	34,253
Operating cost ($)	52,335	35,583
EENS (KWh)	2,015	242
Profit-to-capital ratio	1.81	5.32

The findings presented in Table 3 indicate that, without budget constraints, placing five DGs at buses 57, 60, 61, 64, and 65 leads to a reduction of EENS by 10,026 kWh relative to the baseline. Consequently, the overall expected operating costs of the PDS during EWEs decline by over 80%. Since network reconfiguration is not feasible in case 1, damage to line (06-07) results in the isolation of laterals 4, 5, 7, and 8, along with buses 7-27 in lateral 6, creating an electrical island. In this case, if local loads cannot be met, the cost of load shedding significantly increases. As depicted in Fig. 7, DG installations are predominantly situated at industrial buses, which incur higher penalties for load shedding. This implies that load shedding can be prioritized at residential buses, where the penalties are lower. The RC dispatch results shown in Fig. 6 highlight the vital importance of line (06-07) in the expected operating costs of the PDS, prompting the RC to dispatch from the depot right after the outage triggered by EWE. The results in Table 3 reveal that the considerable investment required for DG installation in case 1 leads to a diminished profit-to-capital ratio compared to the base case. Moreover, since the lines affected by damage must undergo repairs, utilizing DGs does not directly impact the service restoration timeline and repair costs, but it can help mitigate load shedding costs during emergencies.

Here, as an example, the performance of RCs during service restoration in case 1 is evaluated. As shown in Fig. 5, in the case of EWE, 6 lines of the IEEE 69-bus PDS are damaged. According to outage management results of case 1 (see Fig. 6), the distribution lines (06-07) and (56-57) are restored by RC(2), the distribution lines (43-44) and (32-33) are restored by RC(1), and distribution lines (24-25) and (29-30) are restored by RC(3). For example, when line (06-07) is damaged at t=5, RC(2) is immediately dispatched from the depot to repair the line. Then, RC(2) arrives at the line location at t=6 and starts repairing it. At the same time, line (43-44) is damaged by EWE, and RC(1) is dispatched from the depot to repair the line. At t=7, repair work commenced on line (43-44) by RC(1), while distribution lines (32-33) and (24-25) were concurrently damaged due to EWE. Despite RC(3) remaining on standby at the depot, DNO decided to maintain its standby status there due to OSA and the potential for additional critical distribution lines to fail in the coming hours. At t=8, distribution lines (29-30) and (56-57) were

simultaneously damaged. In this situation, DNO has immediately dispatched RC(3) to the location of line (29-30) in lateral 2. At t=10, RC(1) has completed the repairs on line (43-44) and the DNO has dispatched it from there to line (32-33) in lateral 2. At t=11, RC(1) has started the repairs on this line. At the same time, RC(2) has completed the repairs on line (06-07), and this line will be energized at t=12. After energizing line (06-07), RC(2) has been dispatched to line (56-57) in lateral 6 for repairs. At t=13, RC(1) is still busy with the repairs on line (32-33), RC(2) has started the repairs on line (56-57), and RC(3) is on its way to line (24-25). At t=14, the repairs on line (32-33) will be completed, and RC(1) has returned to the depot after energizing that line at t=15. Similarly, the repairs of lines (56-57) and (24-25) were completed at t=16 and t=18, respectively, and RCs 2 and 3 returned to the depot after restoring these lines.

In case 2, the impact of network reconfiguration on outage management is assessed. As shown in Table 3, network reconfiguration in case 2 leads to a decrease in both DGs and RCs when compared to case 1. The planning results in this case demonstrate that network reconfiguration during emergency operations not only lowers expected operational costs but also cuts investment costs. The total annualized costs in case 2 are lowered, and the profit-to-capital ratio in this case surpasses that of case 1. Consequently, integrating network reconfiguration with outage management has proven to be more beneficial for the PDS. The RC dispatch results in case 2 (see Fig. 6) indicate that the reduced number of RCs compared to case 1 leads to an extended service restoration time. Fig. 8 illustrates the planning results for the IEEE 69-bus PDS in case 2.

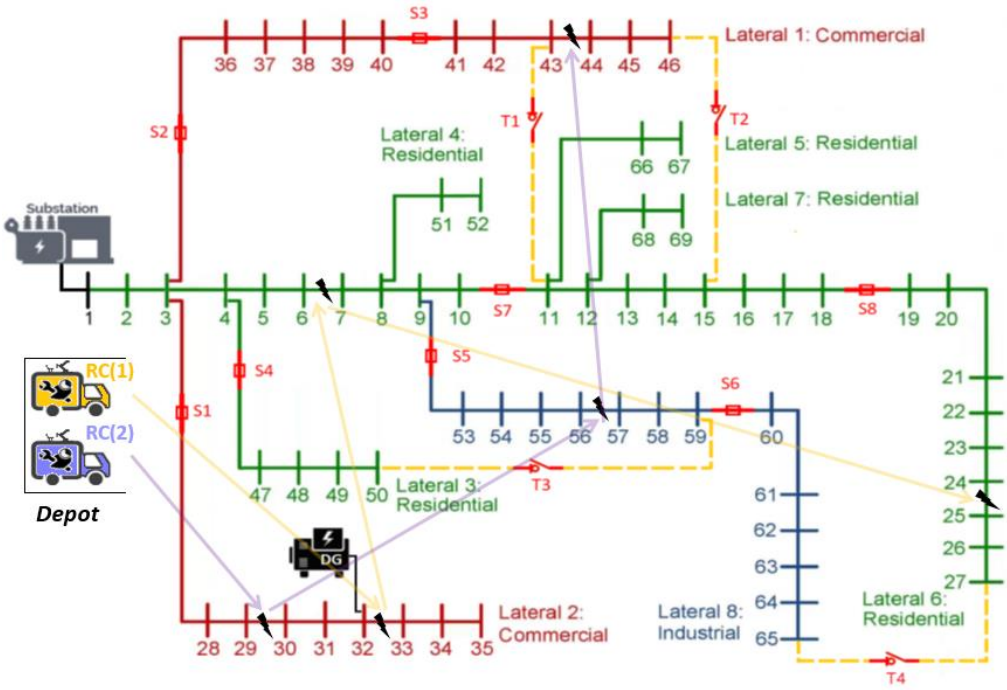

Fig. 8. IEEE 69-bus PDS planning results of case 2.

As illustrated in Figs. 6 and 8, during the preventive operation period, the switches S1-S8 are in the closed state, while the switches T1-T4 on the tie-lines remain open. When the first fault occurs at t=5 on line (06-07), the network's reconfiguration allows the DNO to energize lateral 8 through lateral 3, as well as supply laterals 4-7 via lateral 1. This energization is achieved by closing T1 and T3 and opening S5, all while adhering to radiality constraints. In this configuration, when tie lines 1 and 3 are activated, the load demand of the PDS continues to be met, provided that the line's flow constraints are respected. At t=6, a failure on line (43-44) disrupts the supply route for buses 44-46 in lateral 1. To avert outages at these buses, the DNO closes T2. At t=7, lines (24-25) and (32-33) experience damage from EWE, prompting the DNO to close T4 to maintain service at buses 25-27 in lateral 6, while buses 33-35 become disconnected from the network. Due to the high cost of load shedding in commercial areas, at t=7, RC(1) is immediately

dispatched from the depot to lateral 2 to address the issues on line (32-33). At t=8, distribution lines (56-57) and (29-30) suffer simultaneous damage from EWE, presenting a critical challenge for PDS operation, given that repairs on previously affected lines are still pending. Consequently, a section is isolated in lateral 2 following the outage of line (29-30), while buses 30-32 receive power from the DG installed at bus 32. As outages increase in lateral 2, RC(2) is dispatched from the depot to line (29-30) at t=8 to reconnect the isolated area to the grid. At t=10, RC(1) completes repairs on line (32-33) and, upon energizing this line at t=11, is then sent to work on line (06-07). However, load shedding becomes necessary if the total load demand at buses 30-35 surpasses the DG capacity. At t=12, repairs on line (29-30) are finished, and at t=13, the previously isolated area in lateral 2 is reconnected to the network. At this moment, RC(2) is dispatched from line (29-30) to line (56-57), while RC(1) continues to work on line (06-07). As shown in Figs. 6 and 8, at t=18, both lines (06-07) and (56-57) can be energized together, prompting the DNO to open T1 and S5 to maintain radiality. Additionally, at this time, RC(1) is dispatched to line (24-25), while RC(2) is assigned to line (43-44). At t=23, RC(2) successfully energizes line (43-44), after which it returns to the depot, as no other lines remain damaged in the PDS. Meanwhile, the DNO upholds radiality constraints by opening T2. At t=24, line (24-25) is ready to be energized, allowing the DNO to revert the network to its normal optimal operating structure by opening T3 and T4 and closing S5. Ultimately, RC(1) also returns to the depot.

5. Conclusion

This paper proposes a two-stage stochastic MILP model aimed at resilience-oriented PDS planning and outage management based on operational situation awareness. The operational situation awareness is derived from the predictability of EWEs, enabling preventive actions to mitigate potential damage. Considering the DNO's capabilities in the resilience assessment process, the approach yields a more accurate evaluation of PDS resilience, facilitating improved enhancement and expansion strategies. The first stage of the proposed model focuses on minimizing investment costs associated with preventing load shedding and ensuring the necessary fast service restoration equipment following EWEs. The second stage targets the minimization of expected operational costs while accounting for operational constraints. The operation period consists of two consecutive sub-periods: a preventive operation period and an emergency operation period. During the preventive operation period, the DNO readies the system for the impending event through reconfiguration and optimal dispatch of DGs to enhance PDS resilience. In the emergency operation period, network reconfiguration, along with strategic DG and RC dispatch and minimal load shedding, aims to mitigate system degradation.

The proposed model was implemented on the IEEE 69-bus PDS, where multiple numerical simulations with varying operational strategies and conditions demonstrated that integrating operational situation awareness led to reduced investment costs while increasing PDS resilience. Given that PDS resilience to EWEs mainly relies on DNO actions pre- and during the events, emphasizing this aspect enhances the model's fidelity and accuracy in assessing resilience. Consequently, integrating operational situation awareness helps avoid unnecessary investments and strengthens system resiliency. By dividing PDS loads into three types with distinct load shedding penalties, investment can be directed to minimize shedding in industrial and commercial sectors, necessitating mandatory load shedding solely for residential buses, which incur lower penalties. Furthermore, in the outage management strategy, priority is given to repairing damaged lines in industrial and commercial areas to minimize the load that remains unsupplied.

Nomenclature

Sets and Indices:

∂^{B}	1-	Set of lines indices l
∂^{C}	2-	Set of RC indices c
∂^{G}	3-	Set of buses with DG ($\partial^{G} \subset \partial^{N}$)
∂^{L}	4-	Set of load buses ($\partial^{L} \subset \partial^{N}$)
∂^{N}	5-	Set of buses indices n and m
∂^{PCC}	6-	Set of substation buses ($\partial^{PCC} \subset \partial^{N}$)
∂^{S}	7-	Set of scenario indices s
∂^{SW}	8-	Set of lines with RCS ($\partial^{SW} \subset \partial^{B}$)
$\partial^{Tp}/\partial^{Te}$	9-	Set of preventive/emergency operation period indices t

Variables:

$C_o(s)$	10- Expected operating cost of scenario *s* ($)
$P_{n,t}^{g,s}$ / $Q_{n,t}^{g,s}$	Active/reactive power generated by DG n at time t (KW/ KVAR)
$P_{n,t}^{gr,s}$ / $Q_{n,t}^{gr,s}$	Active/Reactive power received from PCC at time *t* (KW/KVAR)
$P_{l,t}^{s}$ / $Q_{l,t}^{s}$	Active/reactive power flow from bus *n* to bus *m* at time t (KW/KVAR)
$v_{n,t}^{s}$ / $v_{m,t}^{s}$	Voltage magnitude of bus *n/m* at time *t*
$\gamma_{n,t}^{L,s}$	Load shedding value of bus *n* at time *t*
ζ^{rc}	Number of required RCs
Binary Variables:	
$\tau_{l,t}^{r,s}$	1 if line l at time *t* is being repaired; 0 otherwise
ζ_n^g	1 if bus n is selected for installing DG; 0 otherwise
Z_c^{RC}	1 if RC(*c*) is equipped; 0 otherwise
$\pi_{l,t}^{s}$	1 if the status of line l is ON at time *t*; 0 otherwise
$\chi_{l,t}^{r,s}$	1 if the RCS on line l is open at time *t*; 0 otherwise
$\chi_{c,l,t}^{s}$	1 if RC(c) is assigned to repair line *l* at time *t*; 0 otherwise
$\omega_{mn,t}^{s}$ / $\omega_{nm,t}^{s}$	1 if *n*/*m* is the parent node of *m*/*n*; 0 otherwise
Parameters:	
B_R	11- Available budget ($)
B_{rc}	12- Available budget for RC allocation ($)
B_{dg}	13- Available budget for DG installation ($)
C_n^g	14- Cost of DG operation at bus *n ($/KWh)*
C_n^{gr}	15- Cost of purchasing power from the upstream network ($)
C_n^L	16- Load shedding cost of bus *n ($/KWh)*
C^{CL} / C^{RL} / C^{IL}	17- Load shedding cost in a commercial/ residential/industrial bus *($/KWh)*
C_l^r	18- Repair cost of line *l ($/hr).*
C^{DG}	19- Annualized cost of a DG ($)
C^{RC}	20- Annualized cost of an RC ($)
D	21- Average occurrence of EWE in a year
$P_n^{g,\max}$ / $Q_n^{g,\max}$	22- Maximum active/reactive power limit of DG n (KW/KVAR)
$P_l^{\max}$ / $Q_l^{\max}$	Maximum active/reactive power limit of line l (KW)
$P_{n,t}^{L,s}$ / $Q_{n,t}^{L,s}$	Active/reactive load demand of bus n at time t (KW/ KVAR)
$P(s)$	Probability of occurrence of scenario *s*
R_l / X_l	Resistance/reactance of line l *(pu)*
$T_l^R(s)$	Time required for washing and repair of line *l* in scenario s
$T_l^T(s)$	Time required to arrive at line *l* in scenario s
$T_c^{\max}$	Max operation time of an RC
V_0	Reference voltage magnitude (pu)
α_n^L	Load importance factor at bus *n*
$\delta_{l,t}^{S}$	1 if line l is ON at time t; 0 otherwise
x_n^{CL} / x_n^{IL} / x_n^{RL}	1 if bus *n* supplies a commercial/ industrial/ residential load; 0 otherwise
ϕ_l^r	1 if line l has existing RCS; 0 otherwise
Δt	Time interval (hr)
Δv	Permissible voltage deviation (pu)

References

[1] President's Council of Economic Adviser, "Economic benefits of increasing electric grid resilience to weather outages", Executive Office President, Washington, DC, USA, Rep., Aug. 2013.

[2] R. J. Campbell, "Weather-related power outages and electric system resiliency", Congr. Res. Serv., Washington, DC, USA, Rep. R42696, Aug. 2012.

[3] A. R. Berkeley, M. Wallace, "A framework for establishing critical infrastructure resilience goals", Nat. Infrastruct. Advisory Council, Washington, DC, USA, Rep., Oct. 2010.

[4] Q. Zhang, Z. Wang, S. Ma, A. Arif, "Stochastic pre-event preparation for enhancing resilience of distribution systems", Renew. Sustain. Energy Rev., Vol. 152, Dec. 2021, Art. no. 111636.

[5] M. Haghshenas, R-A. Hooshmand, M. Gholipour, "A novel cost-based optimization model for electric power distribution systems resilience improvement under dust storms", Int. J. Crit. Infr. Pro., Vol. 44, Mar. 2024, Art. no. 100659.

[6] M. Haghshenas, R-A. Hooshmand, M. Gholipour, "Power Distribution System Resilience Enhancement Planning against Extreme Dust Storms via Pre- and Post-Event Actions Considering Uncertainties", Sust. Cit. Soc., Vol. 78, Mar. 2022, Art. no. 103626.

[7] M. Haghshenas, R-A. Hooshmand, M. Gholipour, "Power distribution system resilience to extreme dust storms: Probabilistic impact assessment and hardening planning", Sust. Res. Infr., Vol. 10, No. 1, pp. 40-62, May 2024.

[8] W. Yuan, J. Wang, F. Qiu, C. Chen, C. Kang, B. Zeng, "Robust optimization-based resilient distribution network planning against natural disasters", IEEE Trans. Smart Grid, Vol. 7, No. 6, pp. 2817–2826, Nov. 2016.

[9] S. Ma, B. Chen, Z. Wang, "Resilience enhancement strategy for distribution systems under extreme weather events", IEEE Trans.

Smart Grid, Vol. 9, No. 2, pp. 1442–1451, Mar. 2018.

[10] X. Wang, Z. Li, M. Shahidehpour, C. Jiang, "Robust line hardening strategies for improving the resilience of distribution systems with variable renewable resources", IEEE Trans. Sustain. Energy, Vol. 10, No. 1, pp. 386–395, Jan. 2019.

[11] M. Salimi, M.-A. Nasr, S. H. Hosseinian, G. B. Gharehpetian, M. Shahidehpour, "Information gap decision theory-based active distribution system planning for resilience enhancement", IEEE Trans. Smart Grid, Vol. 11, No. 5, pp. 4390–4402, Sep. 2020.

[12] H. Zhang, S. Ma, T. Ding, Y. Lin, M. Shahidehpour, "Multistage multi-zone defender-attacker-defender model for optimal resilience strategy with distribution line hardening and energy storage system deployment", IEEE Trans. Smart Grid, Vol. 12, No. 2, pp. 1194–1205, Mar. 2021.

[13] C. He, C. Dai, L. Wu, T. Liu, "Robust network hardening strategy for enhancing resilience of integrated electricity and natural gas distribution systems against natural disasters", IEEE Trans. Power Syst., Vol. 33, No. 5, pp. 5787–5798, Sep. 2018.

[14] X. Wang, M. Shahidehpour, C. Jiang, and Z. Li, "Resilience enhancement strategies for power distribution network coupled with urban transportation system", IEEE Trans. Smart Grid, Vol. 10, No. 4, pp. 4068–4079, Jul. 2019.

[15] S. Ma, L. Su, Z. Wang, F. Qiu, G. Guo, "Resilience enhancement of distribution grids against extreme weather events", IEEE Trans. Power Syst., Vol. 33, No. 5, pp. 4842–4853, Sep. 2018.

[16] S. Ma, S. Li, Z. Wang, F. Qiu, "Resilience-oriented design of distribution systems", IEEE Trans. Power Syst., Vol. 34, No. 4, pp. 2880–2891, Jul. 2019.

[17] Y. Tan, A. K. Das, P. Arabshahi, D. S. Kirschen, "Distribution systems hardening against natural disasters", IEEE Trans. Power Syst., Vol. 33, No. 6, pp. 6849–6860, Nov. 2018.

[18] M. Haghshenas, R-A. Hooshmand, M. Gholipour, "Simultaneous hardening planning of lines and substations for resilience enhancement of electric power distribution system against dust storms", Ir. Elec. Ind. J. Quality and Prod., Vol. 11, No. 3, pp. 48-61, Sep. 2022.

[19] M. Movahednia, A. Kargarian, C. E. Ozdemir, S, C. Hagen, "Power grid resilience enhancement via protecting electrical substations against flood hazards: A stochastic framework", IEEE Trans. Ind. Inf., Vol. 18, No. 3, pp. 2132-2143, Mar. 2022.

[20] H. Wang, T. Jin, "Prevention and survivability for power distribution resilience: A multi-criteria renewables expansion model", IEEE Access, Vol. 8, pp. 88422–88433, 2020.

[21] K. S. A. Sedzro, A. J. Lamadrid, L. F. Zuluaga, "Allocation of resources using a microgrid formation approach for resilient electric grids", IEEE Trans. on Power Syst., Vol. 33, No. 3, pp. 2633-2643, May 2018.

[22] S. Ghasemi, J. Moshtagh, "Distribution system restoration after extreme events considering distributed generators and static energy storage systems with mobile energy storage dispatch", Applied Energy, Vol. 310, Mar. 2022, Art. No. 118507.

[23] J. Yan, B. Hu, K. Xie, T. Niu, C. Li, H. Tai, "Dynamic repair scheduling for transmission systems based on look-ahead strategy approximation", IEEE Trans. Power Syst., Vol. 36, No. 4, pp. 2918-2933, July, 2021.

[24] A. Arif, S. Ma, Z. Wang, J. Wang, S. M. Ryan, C. Chen, "Optimizing service restoration in distribution systems with uncertain repair time and demand", IEEE Trans. Power Syst., Vol. 33, No. 6, pp. 6828-6838, Nov. 2018.

[25] T. Ding, Z. Wang, W. Jia, B. Chen, C. Chen, M. Shahidehpour, "Multiperiod distribution system restoration with routing repair crews, mobile electric vehicles, and soft-open-point networked microgrids", IEEE Trans. Smart Grid, Vol. 11, No. 6, pp. 4795-4808, Nov. 2020.

[26] W. Tang, Z. Li, Z. Yu, T. Qian, X. Lian, X. Chen, "Cost-optimal operation and recovery method for power distribution systems considering multiple flexible resources and logistics restrictions", Sust. Energy Tech. Ass., Vol. 49, Feb. 2022, Art. no. 101761.

[27] M. Haghshenas, R-A. Hooshmand, M. Gholipour, "Stochastic resilience enhancement planning for electric power distribution systems against extreme dust storms", Ir. J. Elec. Comp. Eng., Vol. 20, No. 2, pp. 108-120, Aug. 2022.

[28] C. Shao, M. Shahidehpour, X. Wang, X.

Wang, B. Wang, “Integrated planning of electricity and natural gas transportation systems for enhancing the power grid resilience”, IEEE Trans. Power Syst., Vol. 32, No. 6, pp. 4418–4429, Nov. 2017.

[29] M. R. Ensley, “Toward a theory of situation awareness in dynamic systems”, Human Factors, Vol. 37, No. 1, pp. 32–64, 1995.

[30] F. Rajaei, M. A. Latify, A. Ebrahimi, “Incorporating DSO’s situational awareness in resilience-oriented distribution system planning”, IEEE Trans. Smart Grid, Vol. 14, No. 3, pp. 1958-1997, May 2023.

[31] Y. Wang, C. Chen, J. Wang, R. Baldick, “Research on resilience of power systems under natural disasters—A review”, IEEE Trans. Power Syst., Vol. 31, No. 2, pp. 1604–1613, Mar. 2016.

[32] Global inflation rate from 2016 to 2026, 2021. Retrieved from: https://www.statista.com

[33] S. Yin, C. Lu, “Distribution feeder scheduling considering variable load profile and outage costs”, IEEE Trans. Power Syst., Vol. 24, No. 2, pp. 652-660, May 2009.